Geochemical Journal, Vol. 50, 2016 doi:10.2343/geochemj.2.0397

Indication of hydrothermal deposits and ore area on caldera floor and shallow sub-seafloor of the Bayonnaise knoll, based on high-resolution acoustic investigation

MIHO ASADA,[1]* TAKAFUMI KASAYA,[1,2] KEIZO SAYANAGI[3] and TADA-NORI GOTO[4]

[1]Research and Development Center for Earthquake and Tsunami, Japan Agency for Marine-Earth Science and Technology (JAMSTEC), 2-15 Natsushima, Yokosuka, Kanagawa 237-0061, Japan
[2]Strategic Innovation Promotion Programs (SIP), Project Team for Development of New-generation Research Protocol for Submarine Resources, JAMSTEC, 2-15 Natsushima, Yokosuka, Kanagawa 237-0061, Japan
[3]Institute of Oceanic Research and Development, Tokai University, 3-20-1, Orido, Shimuzu-ku, Shizuoka 424-8610, Japan
[4]Department of Civil and Earth Resources Engineering, Kyoto University Graduate School of Engineering, Kyoto Daigaku-katsura, Nishikyo-ku, Kyoto 615-8540, Japan

(*Received February 4, 2015; Accepted October 13, 2015*)

The Bayonnaise knoll, an active submarine volcano belonging to an actively rifted part of the Izu-Bonin volcanic arc, exhibits hydrothermal ore deposits on its caldera floor in a region known as the Hakurei Sulfide Deposit (HSD) area. We observed the HSD area using high-resolution acoustic observation equipment consisting of multibeam echo sounder (MBES), sidescan sonar (SSS), and sub-bottom profiler (SBP) systems, on the AUV *Urashima*. We used visual and acoustic results to examine the consistency of the HSD area extent and to consider possibilities of other ore areas within the caldera. The resultant high-resolution acoustic imageries suggest expansion of the HSD area to the northeastern caldera wall and the southwestern sub-seafloor of the caldera floor. The SBP data show a thick sediment layer on the western part of the caldera floor where many high-backscattering signals were observed. Small chimney-like features were acoustically observed in the HSD area and also at the central cone and along the rim of the caldera. However, most are remnant features of ancient volcanic activity of the knoll, and thus may not indicate current hydrothermal deposits. Acoustic investigations such as this, along with appropriate interpretation, are very useful to determine the detailed distribution of ore on the seafloor and at the shallow subsurface, and should be an effective tool for regional site surveying before seabed mineral mining.

Keywords: hydrothermal deposits, high-resolution acoustic observation, AUV, sub-seafloor, SBP

INTRODUCTION

Because hydrothermal fields are frequently accompanied by ore deposits, they have been investigated for the pursuit of economic value in addition to scientific interests. In general, repeated investigations by conventional methods such as shipboard bathymetric surveys, tow-yo surveys, visual observation, and by incidental discovery of hydrothermal fields are needed to discover and map hydrothermal fields and ore deposits on the vast oceanic floor. High-resolution acoustic investigation using autonomous underwater vehicles (AUVs) has been recently used to discover and map hydrothermal sites (German *et al*., 2008; Kumagai *et al*., 2010; Nakamura *et al*., 2013) because this method is effective for determining the distribution details of hydrothermal structures on the seafloor and in shallow depths of the sub-seafloor at a scale of several meters.

The Bayonnaise knoll is an active submarine volcano in an actively rifted section along the west side of the Izu-Bonin volcanic arc (Honza and Tamaki, 1985; Tayler *et al*., 1990). The Bayonnaise knoll is located at 31°57–58′ N, 139°25–45′ E on the eastern edge of the Shikoku basin on the Philippine Sea Plate (Fig. 1). A large hydrothermal ore deposit known as the Hakurei Sulfide Deposit (HSD) was discovered on an inner wall of the caldera of the Bayonnaise knoll by the Japan Oil, Gas and Metals National Corporation (JOGMEC) in 2003 (Tanahashi *et al*., 2006). The ore on the seafloor and its detailed distribution were confirmed by visual observation and temperature mapping by a deep-tow camera, a finder-mounted Power Grab TV system, and Conductivity Temperature Depth (CTD) sensors (Iizasa *et al*., 2004; Tanahashi *et al*., 2006, 2008). The geometrical characteristics of the

*Corresponding author (e-mail: asadam@jamstec.go.jp)

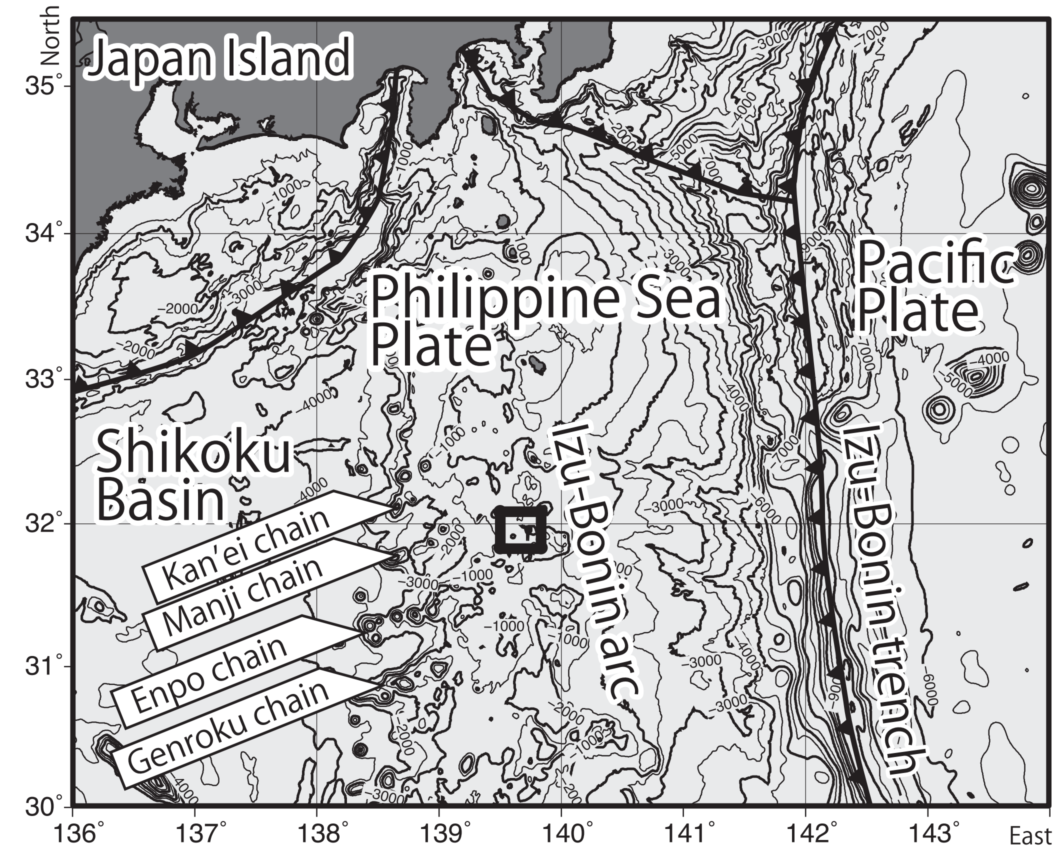

Fig. 1. Bathymetry map of part of the Izu-Bonin volcanic arc drawn from JTOPO30 data (gridding data, Marine Information Research Center, Japan Hydrographic Association, 2003). Contour interval is 500 m. Inset indicates position of Fig. 2.

Bayonnaise knoll and its caldera and surrounding seamounts are similar to those of the Hokuroku basin, which is the largest site of Kuroko ore deposits on land that is considered to be ancient hydrothermal deposits in an environment of stagnant seawater of a submarine volcano in Japan (Nakajima, 1993; Terakado, 2001; Tanahashi *et al*., 2008). Thus, in situ observation of the developing hydrothermal ore deposits in the caldera of the Bayonnaise knoll is expected to be worthwhile in the near future.

The AUV *Urashima* (JAMSTEC) has three independent acoustic observational instruments including multibeam echo sounder (MBES), sidescan sonar (SSS), and sub-bottom profiler (SBP) systems (Tsukioka *et al*., 2005; Kasaya *et al*., 2011). This vessel is suited to high-resolution acoustic observations because its cylindrical chassis contributes to maintaining a stable attitude during surveys. To compare the ore area on the seafloor determined by our acoustic observation with the distribution of the HSD area reported in 2006 (Tanahashi *et al*., 2006), and to examine unconfirmed ore within the same caldera, we conducted cruises with the AUV *Urashima* and its mother ship R/V *Yokosuka* (YK10-17 and YK11-11; JAMSTEC). Camera observation by the ROV *HyperDolphin* (NT12-20; JAMSTEC) obtained ground reference data along a single survey line, over a part of the acoustically imaged area. Our acoustic investigations provide the planar distribution of ore deposits on the seafloor and continuity in the shallow region under the seafloor, after which detailed geochemical investigation can be conducted to determine the spatial distribution of the ore indicators.

Tectonic Setting of Survey Area

The Pacific Plate subducts under the Philippine Sea Plate ~200 km east of the Bayonnaise knoll along a nearly north-south-trending subduction zone (Fig. 1). The typical geological profile in this area from the trench toward the basin includes the trench, inner trench slope, forearc basement high, forearc basin, volcanic ridge (Izu-Bonin arc), backarc depression, backarc knoll zone, backarc trough and ridge, and backarc (Shikoku) basin (Honza and Tamaki, 1985). Backarc volcanic chains overlie several local portions of the Shikoku basin to the backarc knoll zone. The Bayonnaise knoll belongs to the rift zone,

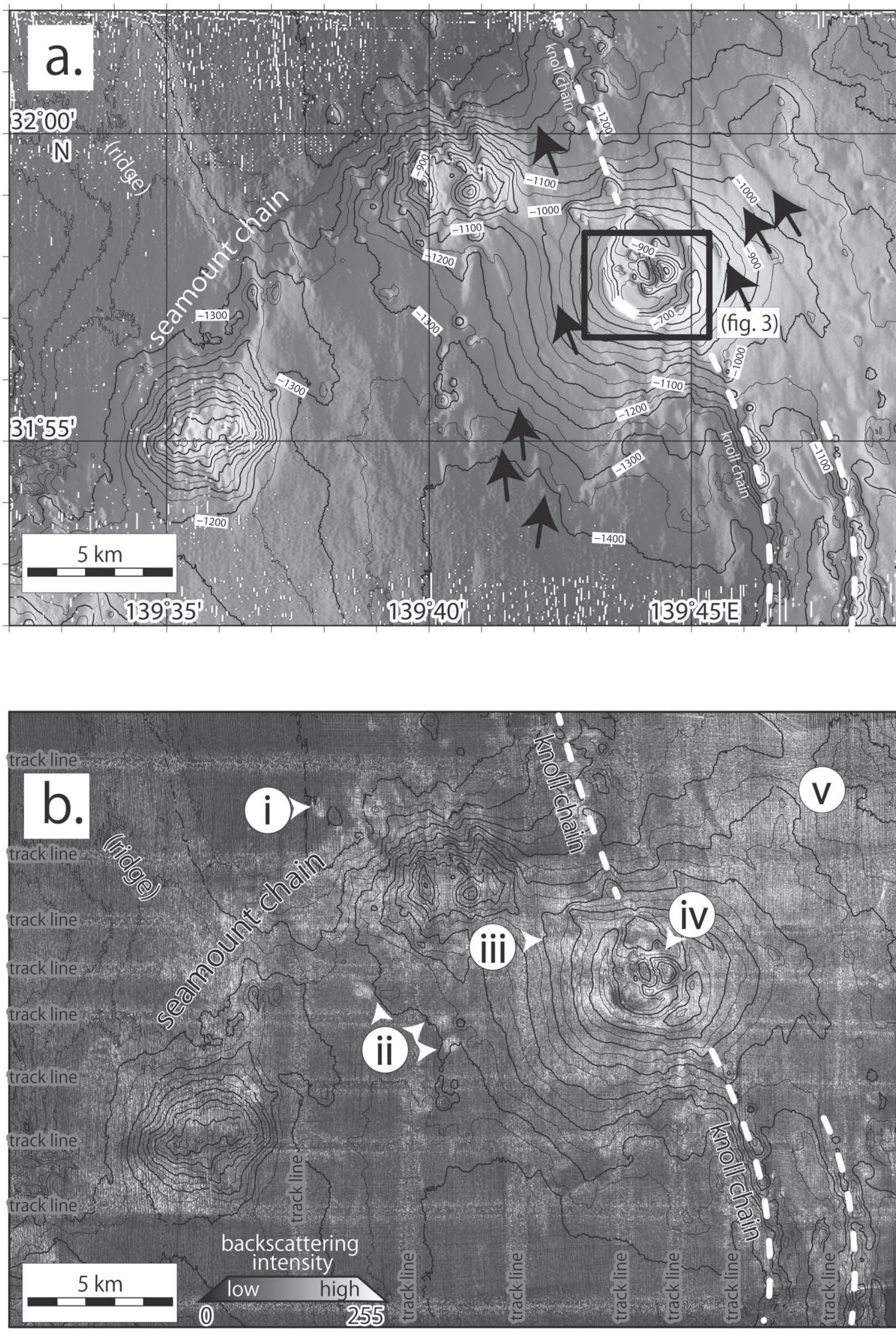

Fig. 2. a: Bathymetry map of Bayonnaise caldera and the surrounding area obtained by R/V Yokosuka (Seabeam 2112). Contour interval is 50 m. Box indicates location of Bayonnaise knoll, shown in Fig. 3. Black arrows indicate linear features interpreted as faults. b: Sidescan sonar image obtained by R/V Yokosuka on bathymetry map (contour interval is 50 m). Black and white shading indicates relative backscattering strength converted to gray scale, with lighter colors indicating higher backscattering intensity. i and ii: conical seamounts located at on and western sides of Bayonnaise knoll, respectively; iii: outer slope of Bayonnaise knoll; iv: central cone of Bayonnaise knoll; v: northeastern seafloor.

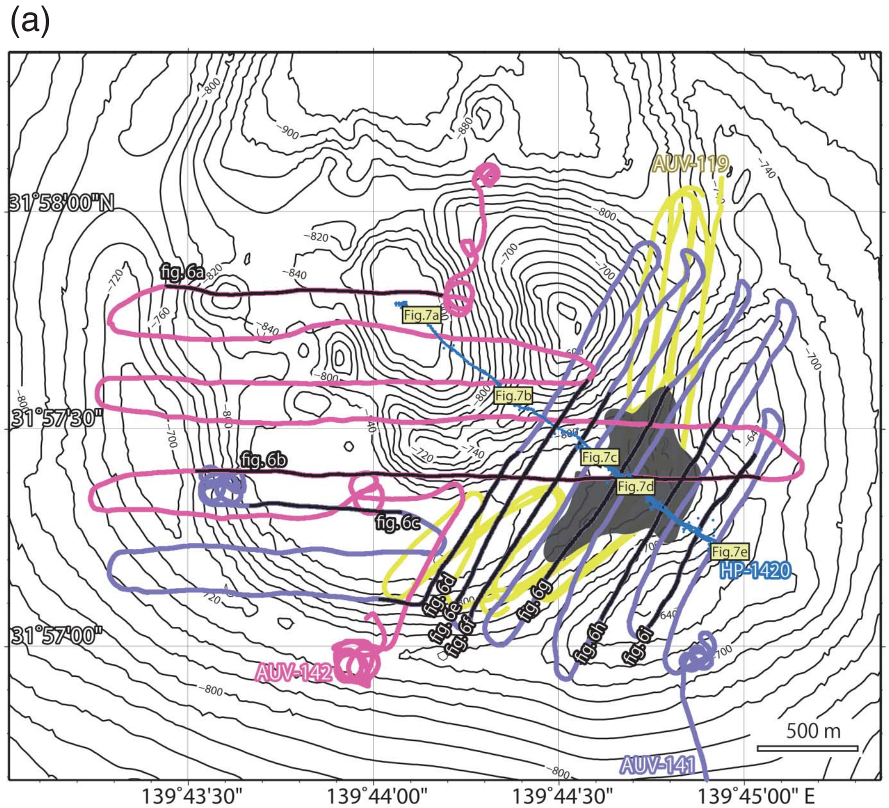

Fig. 3. (a) Survey track lines of autonomous underwater vehicle (AUV) dives #119, 141, and 142 and that of remotely operated vehicle (ROV) 1420 on bathymetry map obtained by R/V Yokosuka. Contour interval is 20 m. Black bold lines on AUV track indicate positions of sub-bottom profiler (SBP) images shown in Fig. 6. Black areas indicate the Hakurei Sulfide Deposit (HSD) area reported in Tanahashi et al. (2006). (b) Bathymetry map of Bayonnaise knoll caldera obtained by R/V Yokosuka overlain by data obtained by AUV Urashima. Contour interval is 5 m. Insets indicate positions of enlarged images in Fig. 5. Black area indicates Hakurei Sulfide Deposit (HSD) area. (c) Geological interpretation map created from sidescan sonar (SSS) imagery. Black bold curve: HSD area proposed by Tanahashi et al. (2006); red bold curve: redrawn ore area in this study, based on facies on SSS imagery and sub-seafloor structures shown by SBP data. Dotted lines: areas observable via SSS (Figs. 4a–c); pale gray color: bathymetry higher than –760 m; slate color: bathymetry deeper than –840 m. Contour interval of background bathymetry is 20 m.

including a part of the backarc knoll zone, which hosts a large number of volcanic knolls (Honza and Tamaki, 1985; Tanahashi *et al*., 2008).

The Shikoku basin and the backarc volcanic chain were active for 26–15 Ma and 17–2.5 Ma (Okino *et al*., 1994; Hochstaedter *et al*., 2000; Ishizuka *et al*., 2002), respectively. The rift zone has been active since 2.5 Ma through the present (Ishizuka *et al*., 2002; Tanahashi *et al*., 2008). The Bayonnaise knoll is situated at the northeastern extension of the Enpo seamount chain, which is a backarc volcanic chain (Figs. 1 and 2). The Myojin knoll caldera and Myojin-sho caldera, as well as other active volcanic knolls known to host hydrothermal activity, belong to a volcanic ridge and are located near the Bayonnaise knoll.

The HSD area is developing at a relatively shallow depth of 680–820 m below the sea surface over an area of 700 m (east-west) × 500 m (north-south) on the seafloor. It is located in a shallow valley, on the easternmost part of the southern caldera floor and in the southeastern part of the inner caldera wall, where the caldera wall curves toward the southeast to form a shallow valley. The HSD area lies at the intersection of the caldera boundary fault and a bathymetrically determined fracture zone (Fig. 2) developing nearly parallel to the Izu-Bonin Arc. Its placement implies that hot water generated by the heat of volcanic activity was emitted through a fault in the caldera wall (Iizasa *et al*., 2004; Tanahashi *et al*., 2008). Honsho *et al*. (2013) reported geomagnetic anomalies over the caldera and high magnetization of the caldera floor, which may have been affected by back-arc-related basaltic volcanism. Honsho *et al*. (2013) also reported weak magnetization at the caldera rim and central cone, which may have been caused by distribution of silicic rock

(b)

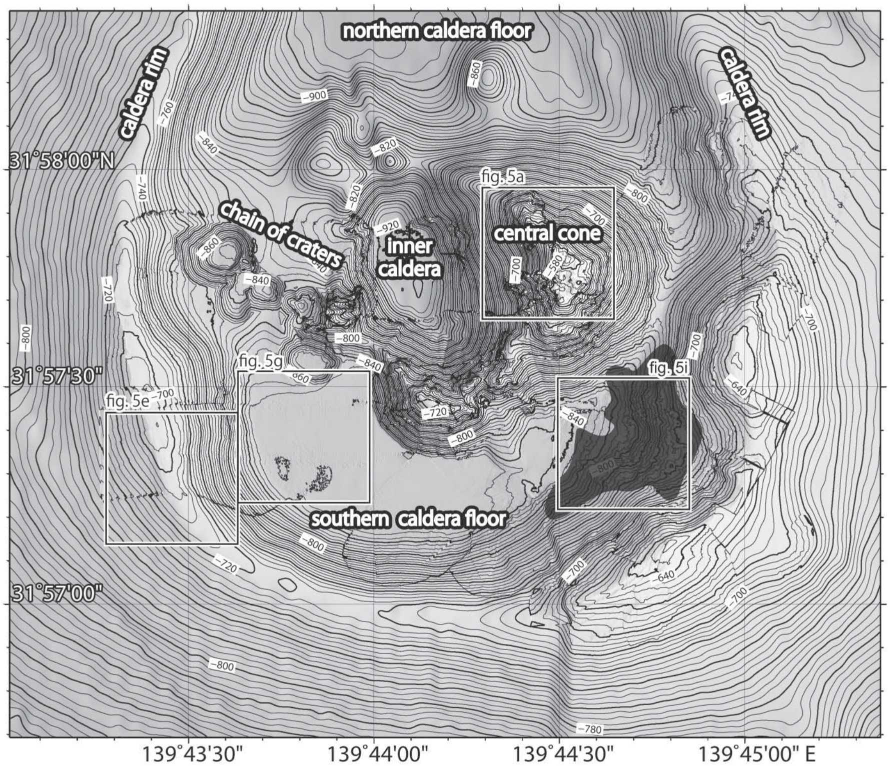

(c)

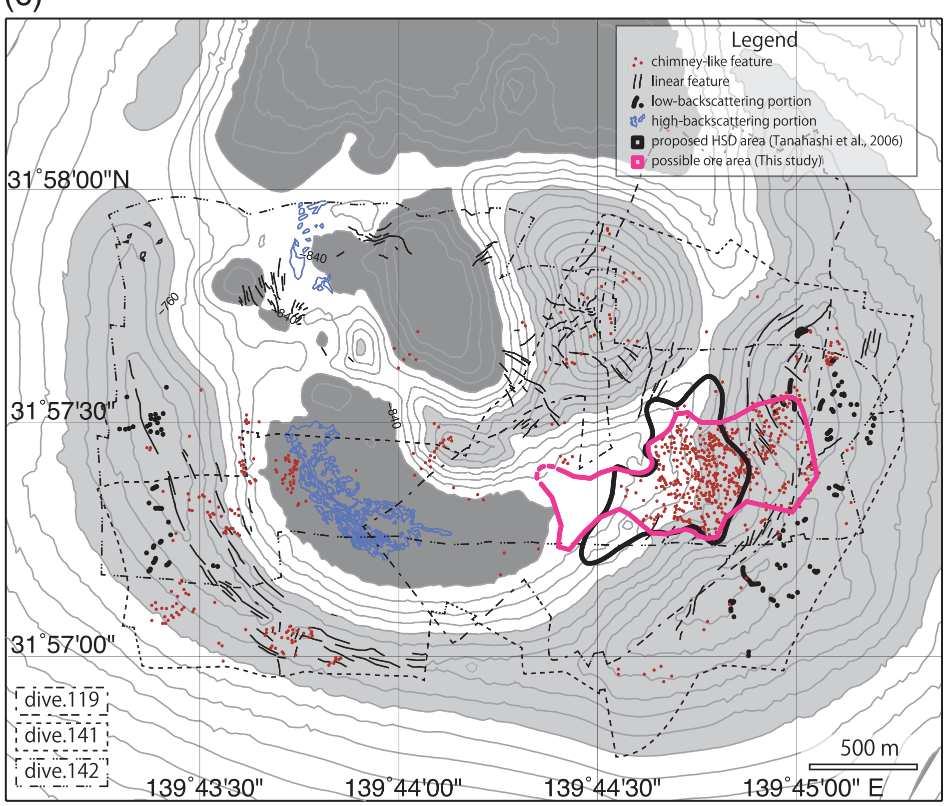

Fig. 3. (continued).

on and around the HSD area, and which may have undergone high-temperature metamorphism affected by the upwelling of hot water along the caldera bounding fault.

Data Acquisition

Shipboard swath-mapping MBES bathymetry data were acquired by a standard hull-mounted SeaBeam 2112 system on the R/V *Yokosuka* (Fig. 3a) that transmits a 12 kHz sonar beam with a swath range of 120°. The meter-scale-resolution bathymetric and SSS data were acquired by the AUV *Urashima*, which was developed in 1998 (Tsukioka *et al.*, 2005; Kasaya *et al.*, 2011). This AUV was preloaded with independent instruments such as a 400 kHz MBES for meter-scale bathymetry data (Fig. 3b), a 120 kHz SSS for backscattering-strength data (Figs. 4a–c and 5), a 1–6 kHz SBP for sub-seafloor information (Fig. 6); a depth meter, an altimeter, and conductivity, temperature, depth, and resolved oxygen (CTDO) sensors.

The AUV *Urashima* generally maintains a stable attitude and navigation, which is especially required for high-resolution acoustic observation using high-frequency acoustic signals. The cruising altitude of the AUV during the two cruises was 100–300 m above the seafloor, and its speed was approximately 2.2 knots. The expected across-track catalogue resolutions were approximately 0.4 cm for the 400 kHz MBES and approximately 7.5 cm for the 120 kHz SSS when the acoustic velocity in seawater was 1500 m/s. The footprint of the along-track acoustic beam was 2–5 m; the beam width was 0.5° for MBES and 0.9° for SSS. An SBP image shows a cross-sectional view and variation of sub-seafloor structures of sediment layers. The cataloged vertical resolution and depth limitation of the SBP observation were several tens of centimeters (Kasaya *et al.*, 2011) and approximately 30 m below the seafloor of sediment layers, respectively. Camera observation by the ROV *HyperDolphin* yielded ground reference images (Fig. 7) along the single track (Fig. 3a).

Survey Results

Observation around Bayonnaise knoll according to wide-range mapping results

Bathymetric features Bathymetric features on and around the Bayonnaise knoll include a seamount chain, which appears to be a northeastern extension of the Enpo seamount chain, approaching the knoll from the northwest (Fig. 2a). Seafloor lineaments trending approximately N30°W are recognized on and around the outer slope of the Bayonnaise knoll. Two lines of knoll chains (sub-parallel to N30°W) are present at the southern side of the Bayonnaise knoll, and a single knoll chain appears on the northern side. Other small knolls are recognized on the western basin floor of the knoll and on the northern side of the seamount chain. A small ridge with a height of ~30 m relative to the surrounding seafloor trends near N30°W on the northern side of the seamount chain.

Features of backscattering strength The backscattering strength data of the MBES signals from the R/V *Yokosuka* were obtained simultaneously with the bathymetry data (Fig. 2b). The backscattering strength data showed relative differences in seafloor material, such as sediment or lava, and gradients, such as a scarp face toward or away from the ship. Therefore, these data are valid for detecting variable geological features such as lava and fault distributions on the seafloor at the kilometer scale.

Relatively higher backscattering signals on the backscattering strength data of the MBES were recognized on the outer slope (Fig. 2b-iii), the central cone (Fig. 2b-iv) of the caldera, and on the northeastern seafloor (Fig. 2b-v) of the Bayonnaise knoll. Other regions showing high backscattering signals included areas along knoll chains and seamount chains in addition to the N30°W-trending small ridge developing on the northern side of the seamount chain. High backscattering signals at the conical seamounts on the northwestern side (Fig. 2b-i) and western side (Fig. 2b-ii) of the Bayonnaise knoll stand out against the surrounding low backscattering signals at the seafloor. These high backscattering signals are planer features, and their regional volcanic activities most likely indicate lava on the seafloor. On the contrary, most of the faults indicated by MBES data near the Bayonnaise knoll caldera are difficult to recognize through shipboard SSS observation. Faults and fissures are linear features visible by SSS observation when fault planes are present. Our result implies that most of fault slopes and the surrounding flat seafloor are covered by sediment exceeding the thickness of the acoustic penetration.

Observation of Bayonnaise knoll caldera using AUV acoustic instruments

The caldera of the Bayonnaise knoll exhibits a characteristic ring-shaped rim approximately 2.8 km diameter in the east-west direction. The rim becomes thick and shallow toward the southeast and thin and deep toward the north (Fig. 3). The shallowest southeastern part of the rim has a depth of 630 m. The central cone lies nearly in the middle of the caldera in the north-south direction and toward the east in the east-west direction; the shallowest depth of the knoll is 570 m. The central cone is part of an inner caldera rim with a diameter of ~900 m. The flat floor of the inner caldera exhibits an ellipsoidal shape with a maximum depth of 920 m. A chain of craters in the form of a series of 4–5 basins lies on the western side of the central caldera. These craters have steep walls and small, flat floors with relative elevations of 20–60 m and dimensions of 300–900 m. The floor of the caldera is divided into northern and southern areas by alignment of the central cone, inner caldera, and the chain of craters (Fig. 3b).

The southern caldera floor shows very small variation in depth. The maximum depth is 850 m, which is ~70 m shallower than the central caldera floor and ~15 m deeper than the HSD area. Conversely, the northern caldera floor shows a narrower, smaller flat seafloor. The northern floor has three individual hills and a wider gentle slope to the central cone toward the south and to the caldera rim toward the east and west, with a maximum water depth of 930 m. Previous research, including our survey, includes the southern caldera floor; however, except for that using an AUV reported by Honsho *et al.* (2013), few observations have been reported for the northern caldera floor.

Observations around HSD

Our AUV *Urashima* observation showed small structures at the center and northeastern side of the "proposed HSD area" (Tanahashi *et al.*, 2006) based on 400-kHz MBES bathymetry data; small structures on the seafloor were identified by acoustic shadows in 120 kHz SSS imagery (Figs. 5i–l). The backscattering intensity was relatively high over the entire proposed HSD area compared to the surrounding seafloor, which indicates local exposure of hard materials on the seafloor. Images obtained by the ROV *HyperDolphin* show transitioning of chimney-like structures increasing from the sediment area to the proposed HSD area (Figs. 7c, 7d1, and 7d2).

Several sub-bottom profiler datasets showed sub-seafloor images from the southern caldera floor toward the proposed HSD area (Figs. 6b, 6g, and 6h), indicating thick and clear sediment layers on the western and central parts of the caldera floor, thinning sediment layers toward the HSD area, and no sediment layers on and near the southwestern side of the proposed HSD area. Figures 6g and 6h show the transected caldera wall and the HSD area. The partially obscured boundary between the seawater and seafloor is considered to be an effect of scattering of acoustic signals at the rough seafloor.

Observation of southern caldera floor

At the western part of southern caldera floor, the bathymetry map shows a few meters of depth variation, and SSS imagery shows many points of high backscattering signals without acoustic shadows (Figs. 5g and 5h); variation in backscattering strength data without bathymetric change is indicative of variation in materials covering seafloor. The points of high backscattering signals on the caldera floor did not reach below the caldera wall. The SBP data showed thick sediment layers (~15 m) in the area covering the rough surface of the bedrock (Figs. 6b and 6c) that continue east of the southern caldera floor (Fig. 6d).

Two outstanding small structures were detected independently by SSS imagery in the central part of the southern basin floor and near the HSD area (Figs. 4a and 4b, arrows). The difference in appearance of the structures between the two SSS imageries (Figs. 4a and 4b) is attributed to differences in slant range or conditions of the SSS system such as setting of gain, imaging contrast, and seawater temperature. Our simultaneous MBES observation did not detect bathymetric features comparable to the two structures (Fig. 3b). The two structures, obscured in the MBES but distinct in the SSS imagery, indicating variation in seafloor material between the structures and surrounding caldera floor. However, the SBP image shows raised bedrock and thus a relatively thin (~10 m thick) sediment layer around these two structures (Fig. 6d). The eastern part of the caldera floor beside the HSD area showed no or few sediment layers (Figs. 6e and 6f).

Central cone

The slopes of the central cone facing east and west showed different facies. The east-facing slope showed a smoother surface with relatively higher backscattering intensity (Figs. 5b–d). The ROV *HyperDolphin* sampled volcanic cobbles covering the top of the central cone (Fig. 7b); no hydrothermal indicators such as biological communities or turbid water were detected. Tanahashi *et al.* (2006) measured the temperature on the eastern slope of the central cone but did not report anomalous results. Small structures on the top and west-facing slope of the central cone were recognized in MBES (Fig. 5a) and SSS images (Figs. 5c and 5d). Iizasa *et al.* (2008) sampled hydrothermal chimneys from the central cone but did not report detailed information such as sampling site or size. Thus, the remaining volcanic and hydrothermal structures may be recognized by our observations on the top and slope of the central cone.

Central caldera

The central caldera, with the basin lying on the west side of the central cone, is covered by thick sediment. The SBP image shows sediment layers more than 15 m thick (Fig. 6a, no bedrock is recognized). The ROV *HyperDolphin* sampled fine-grained sediment by a corer (Fig. 7a). No features of this sediment indicated hydrothermal activities.

Chain of craters

The SSS images indicate several geological linear features on parts of the steep slopes of the chain of craters with relatively low backscattering intensity. No small structures are present; thus, there is no similarity to those of the HSD area. The SBP images show the sub-seafloor structures of the bottoms of the craters (Fig. 6a) with poor clarity owing to side echoes. Other images have not been obtained so far, in this area.

Caldera rim of Bayonnaise knoll

Several points of low backscattering signals without acoustic shadow or spotty bathymetric features were observed along the caldera rim (Figs. 5e and 5f). The SBP images show no sediment layers on the rim (Figs. 6h and 6i); rather, they show a flat, stony seafloor (Fig. 7e1) and seafloor partly covered by thin sediment (Fig. 7e2) based on visual observation from the ROV *HyperDolphin*.

DISCUSSION

Macroscopic geological information of Bayonnaise knoll and surrounding seafloor

High backscattering signals in SSS observations generally suggest the distribution of harder materials on the seafloor, which implies relatively new volcanic activity or bathymetric features facing the sonar (Smith *et al*., 1995; Sauter *et al*., 2002; Cann and Smith, 2005). The shipboard observation of backscattering intensity in the present study indicated relatively high backscattering signals on the outer slope, central cone, northeastern caldera floor of the Bayonnaise knoll, knoll chains, seamount chains, and the N30°W-trending small ridge developing on the northern side of the seamount chain (Fig. 2b). It is noteworthy that conical seamounts showed outstanding signals against the surrounding low backscattering seafloor (Figs. 2b-i and 2b-ii). The high backscattering signals are planar features and imply relatively new volcanism compared to that on the surrounding seafloor. Conversely, backscattering signals were relatively low along faults developing on the northeastern and western part of the outer slopes of the Bayonnaise knoll, suggesting less active faulting in this area.

Coincidence and possible expansion of the HSD area between visual and acoustic observations

Our acoustic observations of the seafloor and subseafloor indicate slightly different distributions of hard materials such as ore deposits in and around the HSD area. Here we use the term "proposed HSD area" for the HSD area presented by Tanahashi *et al*. (2006) and "possible ore area" for our suggested ore distribution, which includes part of the proposed HSD area.

The seafloor covered by hard materials and/or chimney-like features are apparent in SSS and MBES imageries as an area of relatively hard and/or rough seafloor with high backscattering signals. These distributions, however, differ slightly from the proposed HSD area. We did not observe such characteristic facies on the northern and south-southwestern parts of the proposed HSD area (Fig. 3c). On the contrary, the chimney-like features on the seafloor were recognized on the northeastern outer side of the proposed HSD area. We suggest redrawing the ore distribution of the ore area, which is contracted northern and south-southwestern parts of the proposed HSD area, and is expanded toward the northeastern outer side of the proposed HSD area.

The SBP data do not show sediment layers at the HSD area and on the caldera wall. The SBP data show fewer sediment layers over a wider area than the proposed HSD area, particularly for southwestern side of the proposed HSD area, where MBES images show a flat seafloor (Figs. 6e–i). On the contrary, thick sediment layers appear at the western and central part of the southern caldera floor. Based on the variation of the SBP data, we propose that hard material is continuous toward southwestward under seafloor, so that outline of the possible ore area is ex-

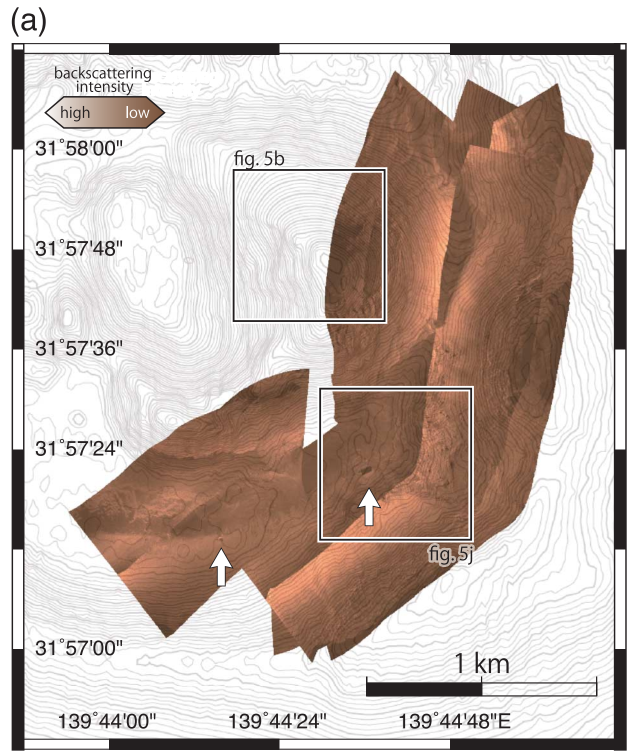

Fig. 4. (a) Sidescan sonar (SSS) image obtained by AUV Urashima dive #119 on bathymetry map (contour interval is 5 m). Insets indicate positions of enlarged images of the SSS images shown in Fig. 5. Arrows indicate positions of small structures on seafloor. (b) Sidescan sonar (SSS) image obtained by AUV Urashima dive #141 on bathymetry map (contour interval is 5 m). Insets indicate positions of enlarged images of SSS images shown in Fig. 5. Arrows indicate positions of small structures on seafloor. (c) Sidescan sonar (SSS) image obtained by AUV Urashima dive #142 on bathymetry map (contour interval is 5 m). Insets indicate positions of enlarged images of the SSS images shown in Fig. 5.

(b)

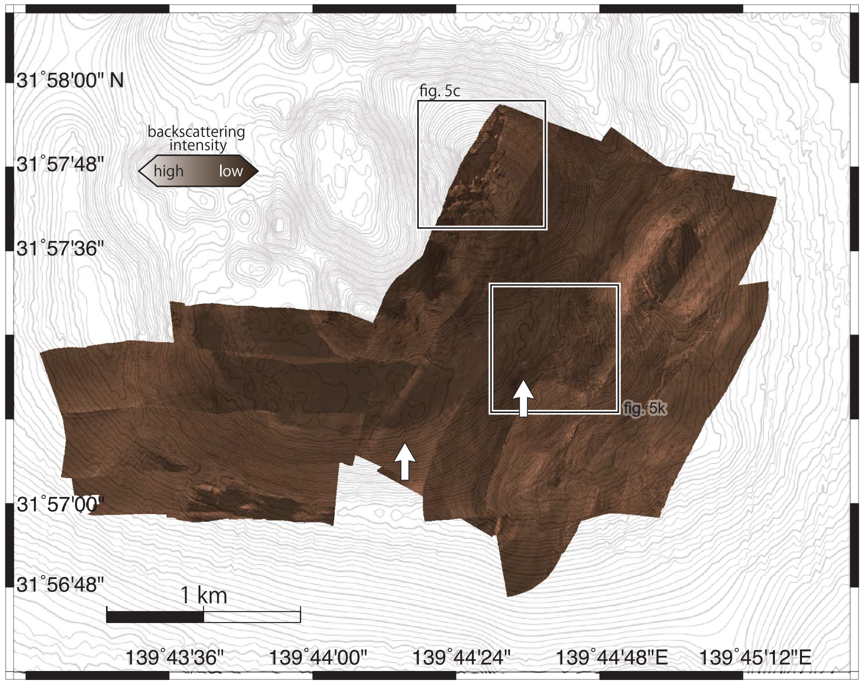

(c)

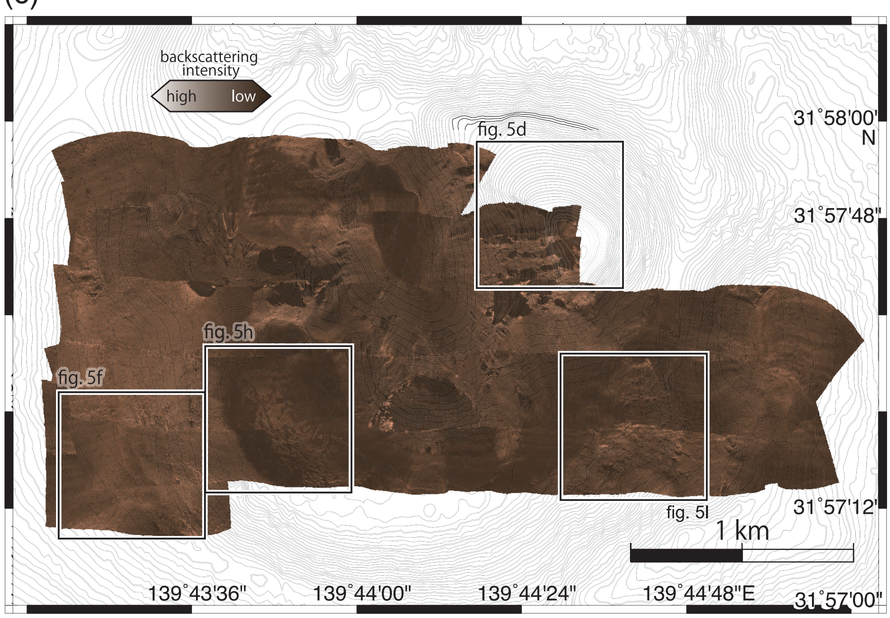

Fig. 4. (continued).

panded toward southwestern outer side of the proposed HSD area (Fig. 3c).

Tanahashi *et al*. (2006) reported temperature anomalies in and around the HSD area including those of +0.1°C (+1.5°C maximum) in a 200 m (east-west) × 500 m (north-south) region and +0.05°C in a region of 1000 m × 600 m (north-south); the defined HSD is 700 m × 500 m. These reports include anomalous rising temperature at a minimum of ~0.05°C on the northeastern side of the HSD area on the eastern caldera wall. Areas without sediment layers in the SBP image along the southwestern side of the HSD area and the southern caldera floor (Figs. 6e and 6f)

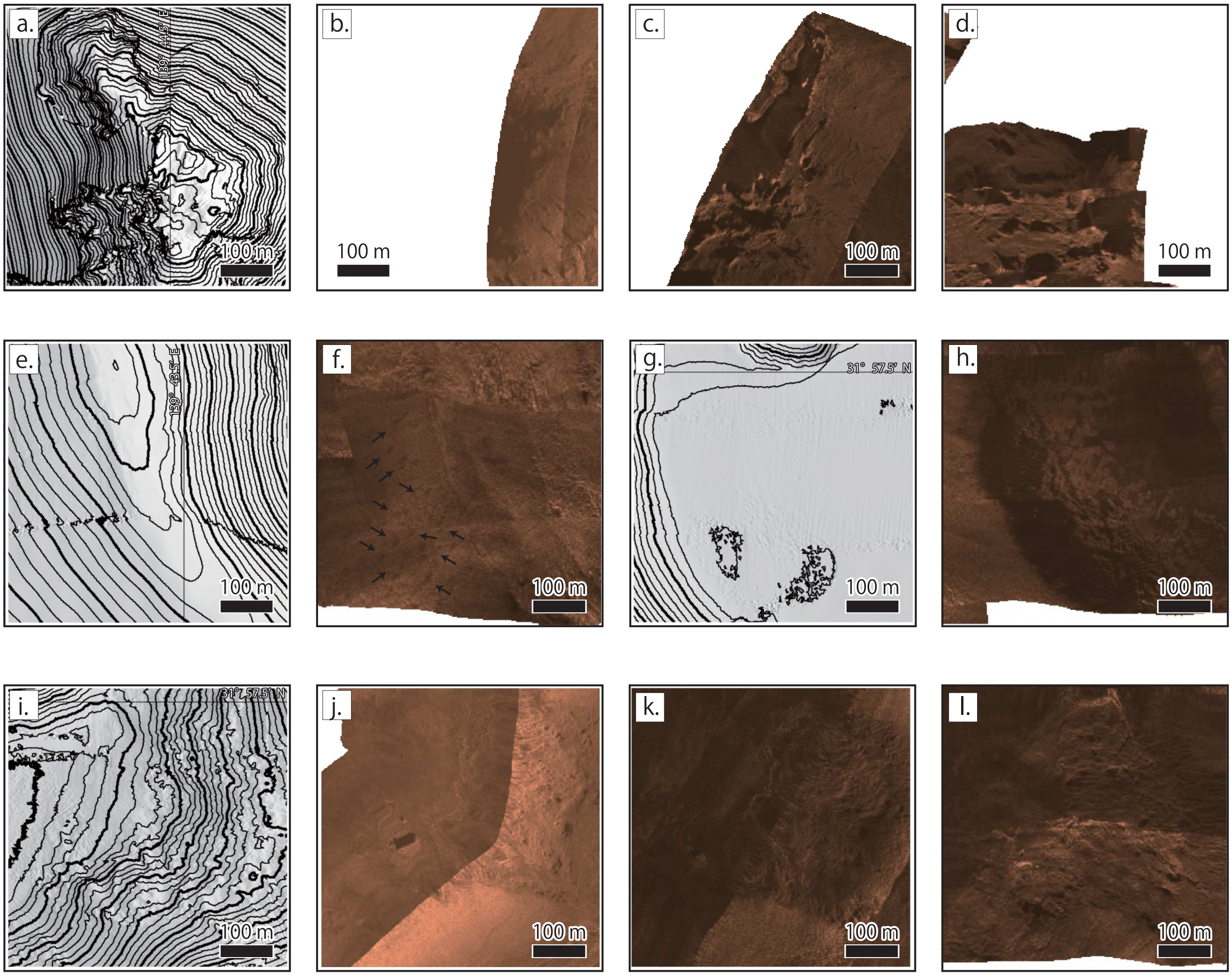

Fig. 5. Enlarged images of bathymetry map and sidescan sonar (SSS) images. Positions of imageries are indicated in Figs. 3 (bathymetry) and 4 (sidescan sonar). a–d: central cone; e and f: caldera rim; g and h: western part of the southern caldera floor; i–l: Hakurei Sulfide Deposit (HSD) area. Black arrows in f indicate spots of low backscattering signals. Contour interval of bathymetry (a, e, g, and i) is 5 m.

partly overlap the area of anomalous rising temperature and cover a wider area than the anomalous area toward the south. Visual observation using the ROV *HyperDolphin* showed a transition of chimney-like structures in a sediment area increasing toward the HSD area. These results indicate that the survey lines of our ROV observation were traced on a relatively consistent boundary among the acoustic imaging and visually proposed HSD area (Fig. 3c).

The reason for the mismatch of outline of the ore area between our opinion and proposed HSD area is the difference in observation methods: our SSS and MBES observations show two-dimensional imaging results, whereas Tanahashi *et al*. (2006) observed by gridded visual surveys using a deep-towed camera and show extrapolating mapping results of chimneys and anomalous temperatures. Particularly for the northeastern side of the HSD area, the outline was drawn by a few survey lines using a deep-towed camera; thus in this case, visual observations may not have been sufficient.

On the basis of the mismatch between the ore area indicated acoustically and the proposed HSD area, we also suggest different distributions between the "structural" ore area and the area of "anomalous temperature". Here the "structural" ore area means a distribution of some hard materials. The area of temperature anomaly should be detected where anomalous fluid are easily transferred, such as a region connected by coarse sediment. In this case, the area of the temperature anomaly is not always accompanied by hard materials. Thus, we assume that the

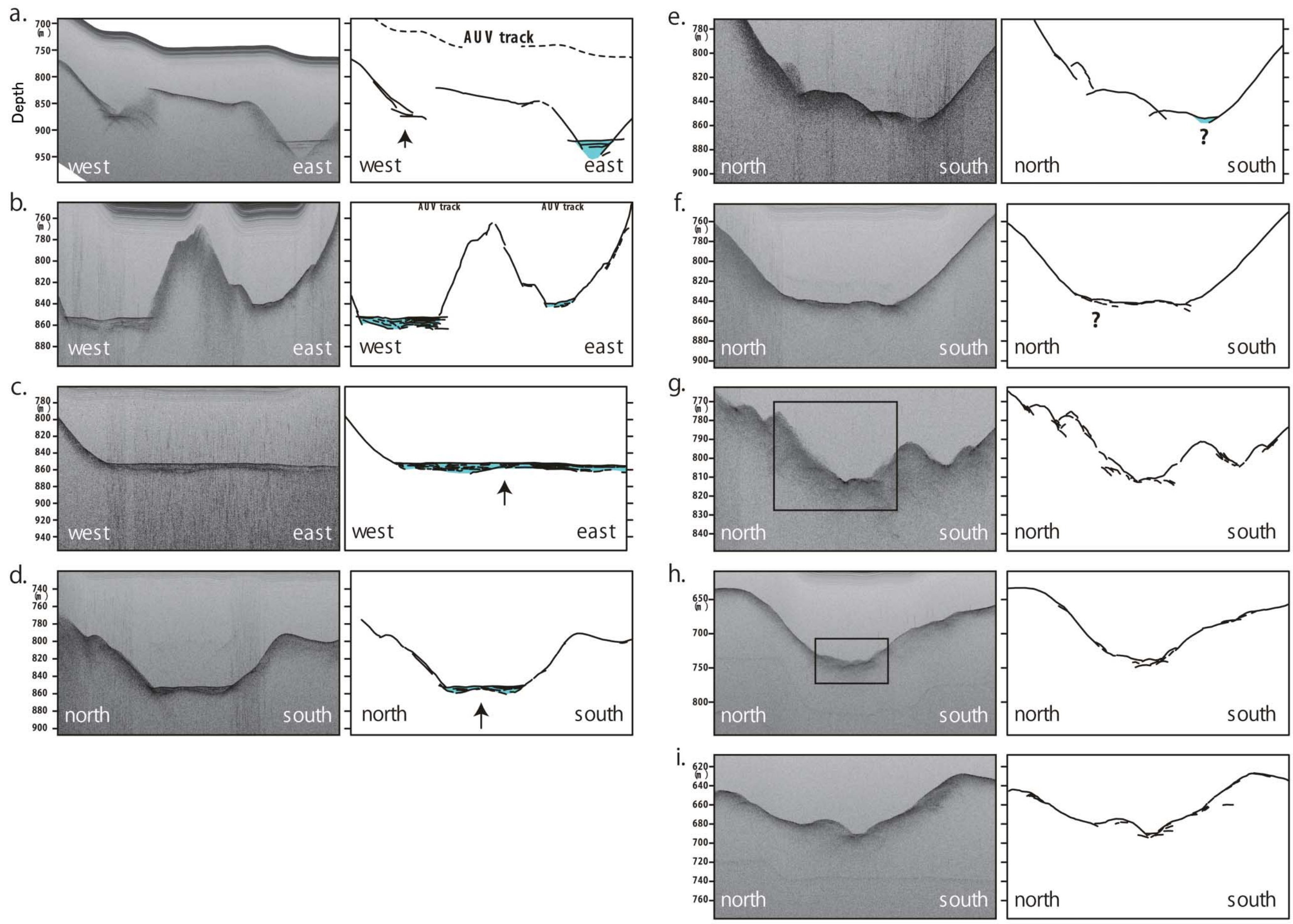

Fig. 6. Left: images of sub-bottom profiler data obtained by the Edgetech 2200 system mounted on the AUV Urashima, and right: interpretation image. Blue area in interpretation image indicates sediment layers. Black arrows indicate raised bedrock. Lines a–i are indicated in Fig. 3a.

HSD area proposed by Tanahashi *et al.* (2006) and our suggested ore area comprise different areas (Fig. 3c). Our acoustic observations indicate the relative hardness of the materials, and cannot separate ore deposits from volcanic rocks. To confirm the real distribution of ore deposits, we need acoustic observations with much higher resolution and/or sub-seafloor sampling, at this stage.

We refrain from discussing the transformation of the ore area between the surveys in 2006 and our surveys in 2010–2012, because of differences in the observation methods. Furthermore, we need more precise evidence, such as flux from hydrothermal activity and growth rates of hydrothermal chimneys, in order to discuss transformation of the ore area. Acoustic observations at lower altitudes would enable finer imaging resolution because of the smaller acoustic signal footprint on seafloor, and also enable deeper acoustic penetration of SBP. High-resolution acoustic observation, which detects fine structures on the seafloor and buried deposits under sediment layers, can contribute to research results for other geophysical investigations.

Yamashita *et al.* (2015) analyzed seismic reflection surveys across the northern part of the Bayonnaise knoll from east to west, and discussed the sub-seafloor structure of the knoll. They report that several faults developing on the eastern flank of the Bayonnaise knoll reach ~1 km below the seafloor, and there are low-velocity zones along the fault zone (Yamashita *et al.*, 2015). The Bayonnaise knoll caldera is an eastern extension of the seamount chain, connecting the northern and southern knoll chains, and there is suspected volcanism (implied by a high-backscattering strength area) on and off the Bayonnaise knoll. This further implies that seawater coming through faults on the eastern Bayonnaise knoll flows down to the detected low-velocity zone (Yamashita *et al.*, 2015), is heated by volcanism, flows up to the seafloor, then forms the HSD area within the caldera of the Bayonnaise knoll. Because of upwelling of heated

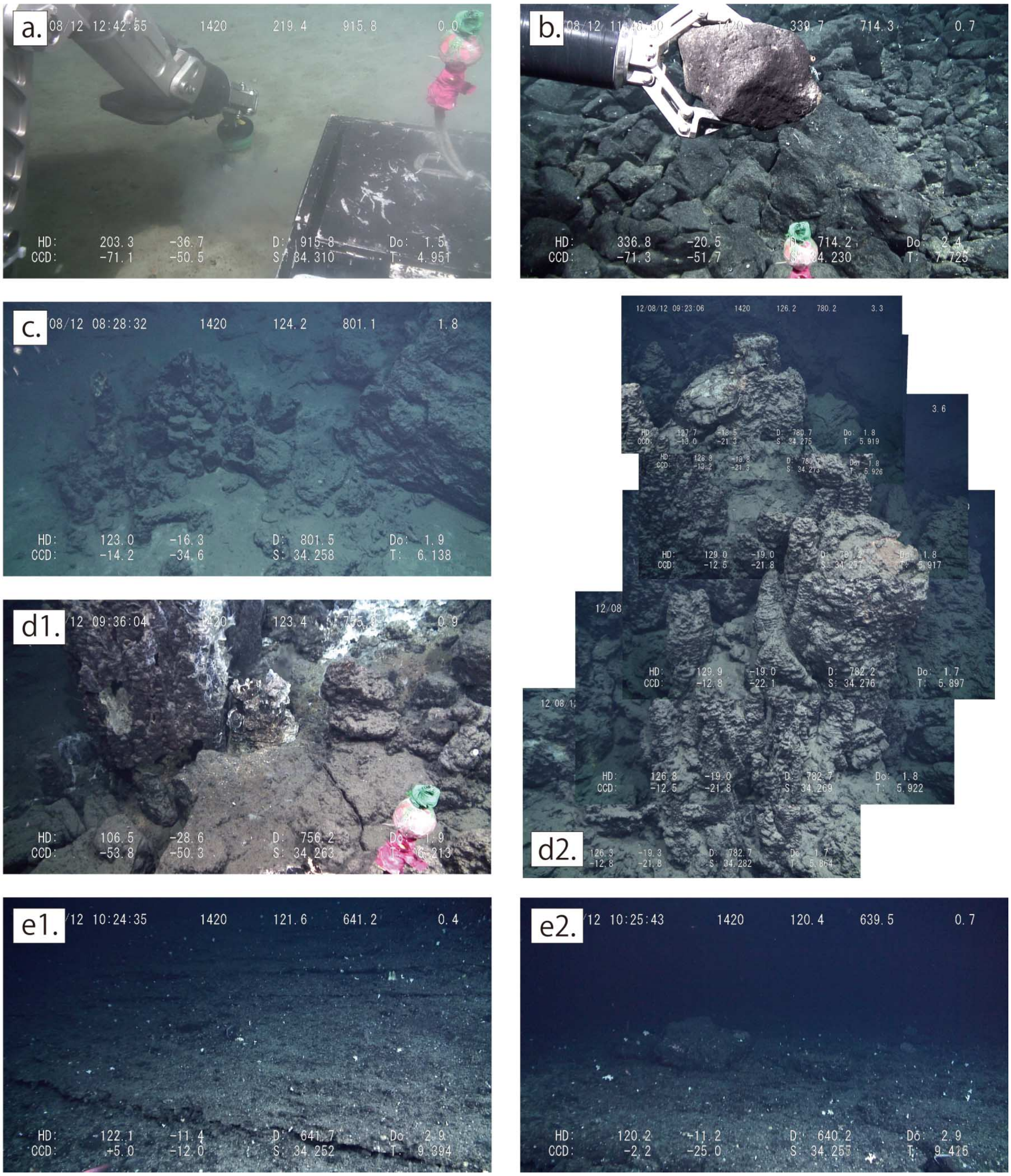

Fig. 7. Seafloor photographs captured by the ROV HyperDolphin. Positions of photographs are indicated in Fig. 3b. a: Monterey Bay Aquarium Research Institute (MBARI) corer on central caldera floor; b: volcanic cobbles on southern slope of central cone; c: chimney or chimney-like structures on easternmost part of the southern caldera floor, which is the western boundary of the reported Hakurei Sulfide Deposit (HSD) area; d1: foot of an active chimney in the HSD area; d2: entire active chimney shown in 4a with an approximate height of 4 m; e1: stony and flat seafloor on caldera rim; e2: part of caldera rim floor slightly covered by sediment.

seawater, Honsho *et al*. (2013) report a relatively weak magnetization zone around the HSD area and propose high-temperature metamorphism of the basaltic volcanic basement rock.

Possible distribution of other hydrothermal sites and ore deposits

Visual observations in the caldera of the Bayonnaise knoll, including our ROV survey, have been very limited thus far, and hydrothermal ore deposits in this caldera have been detected only in the HSD area. An objective of the present research is the search for other ore deposits based on acoustic imaging.

Areas of high backscattering signals occur in the westernmost part of the southern caldera floor, where the bathymetry indicates a very flat area. This result indicates that the high backscattering signals represent hard materials on the surface of the caldera floor and are not effects of bathymetry. In addition, a relatively weak magnetization is present in this region (Honsho *et al*., 2013), and a number of chimney-like features are also indicated in this area by our acoustic observations (Fig. 3c). Sediment layers ~15 m thick (Figs. 6b and 6c) cover the rough surface of the bedrock and continue eastward, as detected by our SBP imagery; within the layers, faulting does not seem to be present (Fig. 6d). This finding indicates that the areas of high backscattering signals are not outcrops of the bedrock. Moreover, it is difficult to consider that these areas are reworked deposits of volcanic rocks from the inner wall of the caldera because these areas appear to be separated from the foot of the inner wall. Visual observation is needed to confirm this feature. Possible origins of hard materials with no bathymetric change on the caldera floor include hydrothermal deposits through metamorphism, biological communities related to seepage from hydrothermal sources below the sediment layers, and pyroclastic materials. If seepage occurs from the bedrock, there is the potential here for other ore deposits independent of those in the proposed HSD area.

Two outstanding structures appear near the proposed HSD area and at the center of the southern caldera floor, where the bedrock is raised and thus the sediment layers are relatively thin. Considering that this structure is exposed volcanic material on the caldera floor, it could be an immature hydrothermal structure. Our recent observation using the new ROV *Kaiko Mark IV* built by JAMSTEC revealed a colored seafloor and turbid seawater in this area (personal communication). Subsequent surveys will include visual observations or coring in this area.

Iizasa *et al*. (2008) reported that they collected a hydrothermal chimney from the central cone in 2007. However, we were unable to detect the characteristics of hydrothermal activity on the eastern slope of the central cone; instead, we observed cobbles by visual observation. Our findings suggest that the central cone is probably an ancient volcanic center not yet covered by thick sediment; thus, the cone could have experienced hydrothermal activity. Our SSS imagery detected small structures on the slope that appear to be similar to those in the proposed HSD area (small structures with high backscattering signals); therefore, some may be hydrothermal structures, and/or bedrock fragmented by the gravitational collapse of the steep slope.

The northern caldera floor is another candidate for hydrothermal ore deposits. Honsho *et al*. (2013) suggested that an additional hydrothermal field may be located in the northwestern part of the caldera at the intersection of the knoll chain and the caldera boundary fault because the geological setting in that area is similar to that in the proposed HSD area. Our shipboard backscattering intensity imagery obtained by the R/V *Yokosuka* showed relatively low backscattering signals over the northern caldera floor. Therefore, it is possible that relatively new hydrothermal fields lie under the northern caldera floor.

Small features are present along the rim of the caldera, particularly on the western and eastern parts of the rim. A patchy pattern of low backscattering signals (Figs. 3c and 5f) and thin sediment (Fig. 6i) were also recognized along the rim. The ROV *HyperDolphin* observation of a limited part of the caldera rim indicated hard rock layers covered with thin sediment (Figs. 7e1 and 7e2). The small features and thin sediment may have been formed by weathering, and no active volcanism and ore along the caldera are expected. The patchy pattern of backscattering signals was also affected by various regional sediment thicknesses as a result of weathering.

Other areas showing low backscattering intensity and thick sediment layers, such as chains of craters and the inner caldera, have less potential for sources of undiscovered hydrothermal deposits.

CONCLUSIONS/SUMMARY

We report highlights of our acoustic observations and comparisons of the acoustic imageries with ground-reference images. A method of high-resolution acoustic observations using AUVs at a roughly focused area via traditional shipboard investigation provide us with detailed two- and three-dimensional geological information, and is effective for exploring ore deposits on the seafloor and in the shallow sub-seafloor. The results of our research can be summarized as follows:

(1) High-resolution acoustic observations using the AUV *Urashima* and visual observations using the ROV *HyperDolphin* were conducted over the southern part of the Bayonnaise knoll caldera. SSS, MBES, SBP, and visual observations detect detailed distribution of small structures, high and low backscattering signals, their ground references, and sub-seafloor sediment layers.

(2) SSS and MBES observations indicated a few chimney-like structures on the northern and south-southwestern parts of the HSD area proposed by Tanahashi *et al*. (2006), and appeared to be continuous toward the northeastern outer side of the proposed HSD area. SBP observations showed sub-seafloor continuity of the ore area toward the southwest. Visual observations by the ROV *HyperDolphin* showed strong correlation of the distribu-

tion of hydrothermal structures on the seafloor with those in the proposed HSD area, along the ROV track. Considering all the observed results, we propose a possible expansion of the HSD area toward the northeast and southwest, and a contraction toward the north and south-southwest directions.

(3) Areas of high backscattering signals on the westernmost part of the southern caldera floor represented hard materials on thick sediment layers. These areas are candidates for hydrothermal deposits through mineralization or for biological communities. Two small structures on the central part of the southern caldera floor and the western slope of the central cone are other candidates related to the distribution of hydrothermal features.

(4) Independent high-resolution acoustic investigations such as SSS, MBES, and SBP by AUVs following shipboard observation can be effective tools for hydrothermal ore research on the seafloor and in the shallow sub-seafloor. These methods are the best techniques for focusing on limited sampling targets followed by visual and sensor observations, and offer efficient exploration in confined areas of ore deposits. Such an area-focused, high-resolution acoustic investigation followed by dense and quantitative investigation, such as geochemical observation, will provide an efficient method for ore discovery and mining.

Acknowledgments—We are grateful for helpful comments from editor, Dr. Kaz Suzuki, and two anonymous reviewers. We thank the Captains and crew of R/V *Yokosuka* and R/V *Natsushima*, the operation teams of AUV *Urashima* and ROV *HyperDolphin*, and supporting members for their cooperation. We are grateful to Dr. Osawa and his group members at MARITEC (Marine Technology and Engineering Center, JAMSTEC) for recent observations by a technical test dive of ROV *Kaiko Mark IV*. Principal funding for this project came from MEXT (Ministry of Education, Culture, Sports, Science and Technology of Japan), in a development program of fundamental tools for exploration of deep seabed resources.

References

Cann, J. R. and Smith, D. K. (2005) Evolution of volcanism and faulting in a segment of the Mid-Atlantic Ridge at 25°N. *Geochem. Geophys. Geosyst*. **6**, Q09008, doi:10.1029/2005GC000954.

German, C. R., Yoerger, D. R., Jakuba, M., Shank, T. M., Langmuir, C. H. and Nakamura, K. (2008) Hydrothermal exploration with the Autonomous Benthic Explorer. *Deep-Sea Res. I* **55**, 203–219.

Hochstaedter, A. G., Gill, J. B., Taylor, B., Ishizuka, O., Yuasa, M. and Morita, S. (2000) Across-arc geochemical trends in the Izu-Bonin arc: Constraints on source composition and mantle melting. *J. Geophys. Res*. **105**, 495–512.

Honza, E. and Tamaki, K. (1985) The Bonin arc. *The Ocean Basins and Margin: 7A The Pacific Ocean* (Nairn, A. E. M., Stehli, F. G. and Uyeda, S., eds.), 459–502, Plenum Press, Now York.

Honsho, C., Ura, T. and Kangsoo, K. (2013) Deep-sea magnetic vector anomalies over the Hakurei hydrothermal field and the Bayonnaise knoll caldera, Izu-Ogasawara arc, Japan. *J. Geophys. Res., Solid Earth* **118**(10), 5147–5164, doi:10.1002/jgrb.50382.

Iizasa, K., Sasaki, M., Matsumoto, K., Shiokawa, S., Tanahashi, M. and on-board scientists (2004) A first extensive hydrothermal field associated with Kuroko-type deposit in a silicic submarine caldera in a nascent rift zone, Izu-Ogasawara (Bonin) Arc, Japan. *Proc. OCEANS'04 MTS/IEEE TECHNO-OCEAN'04*, 991–996.

Iizasa, K., Kojima, S., Okamura, K., Nishimura, K., Kishimoto, K., Shimoda, H., Watanabe, H., Nemoto, S., Yorisue, T., Ishikawa, Y., Goto, K. and Nishikawa, Y. (2008) Preliminary results of NT07-17: hydrothermal ore deposits at and around the Myojin-sho Caldera. Abstract of *BlueEarth'08*, S38 (2008.03.13), Yokohama, Kanagawa, available at http://www.jamstec.go.jp/maritec/j/blueearth/2008/program/pdf/S38.pdf (in Japanese).

Ishizuka, O., Uto, K., Yuasa, M. and Hochstaedter, A. G. (2002) Volcanism in the earliest stage of back-arc rifting in the Izu-Bonin arc revealed by laser-heating ^{40}Ar/^{39}Ar dating. *J. Volcanol. Geotherm. Res*. **120**, 71–85.

Kasaya, T., Kanamatsu, T., Sawa, T., Kinoshita, M., Tukioka, S. and Yamamoto, F. (2011) Acoustic images of the submarine fan system of the northern Kumano basin obtained during the experimental dives of the deep sea AUV URASHIMA. *Exploration Geophys*. **42**, 80–87.

Kumagai, H., Tsukioka, S., Yamamoto, H., Tsuji, T., Shitashima, K., Asada, M., Yamamoto, F. and Kinoshita, M. (2010) Hydrothermal plumes imaged by high-resolution side-scan sonar on a cruising AUV *Urashima*. *Geochem. Geophys. Geosyst*. **11**, 12, doi:10.1029/2010GC003337.

Nakajima, T. (1993) Reconstruction of the depositional circumstances of the kuroko deposits in the Hokuroku basin. *Bull. Geol. Surv. Japan* **44**(2/3/4), 251–282 (in Japanese with English abstract).

Nakamura, K., Toki, T., Mochizuki, N., Asada, M., Ishibashi, J., Nogi, Y., Yoshikawa, S., Miyazaki, J. and Okino, K. (2013) Discovery of a new hydrothermal vent based on an underwater, high-resolution geophysical survey. *Deep-Sea Res. I* **74**(1), 10, doi.org/10.1016/j.dsr.2012.12.003.

Okino, K., Shimakawa, Y. and Nagaoka, S. (1994) Evolution of the Shikoku Basin. *J. Geomag. Geoelectr*. **46**, 463–479.

Sauter, D., Parson, L., Mendel, V., Rommevaux-Jestin, C., Gomez, O., Briais, A., Mevel, C., Tamaki, K. and the FUJI scientific team (2002) TOBI sidescan sonar imagery of the very slow-spreading Southwest Indian Ridge: evidence for along-axis magma distribution. *Earth Planet. Sci. Lett*. **199**, 81–95.

Smith, D. K., Cann, J., Dougherty, M. E., Lin, J., Spencer, S., Macleod, C., Keeton, J., Mcallister, E., Brooks, B., Pascoe, R. and Robertson, W. (1995) Mid-Atlantic Ridge volcanism from deep-towed side-scan sonar images, 25°–29°N. *J. Volcanol. Geotherm. Res*. **67**, 233–262.

Tanahashi, M., Shiokawa, S., Murayama, N. and Takatori, R. (2006) A large hydrothermal sulfide deposit discovered in the Bayonnaise knoll, Izu-Bonin back-arc rift. *Resource Geol*. **56**(2), 185–196 (in Japanese with English abstract).

Tanahashi, M., Fujioka, K. and Machida, S. (2008) Myojin Rift, Izu-Bonin arc as the modern analog of Hokuroku Basin, northeast Japan: Geotectonic significance of the new hydrothermal deposit in the Back-Arc Rift. *Resource Geol*. **58**, 301–312.

Tayler, B., Brown, G., Fryer, P., Gill, J., Hochstaedter, A., Hotta, H., Langmuir, C., Leinen, M., Nishimura, A. and Urabe, T. (1990) ALVIN-SeaBeam studies of the Sumisu rift, Izu-Bonin arc. *Earth Planet. Sci. Lett*. **100**, 127–147.

Terakado, Y. (2001) Re-Os dating of the Kuroko ore deposits from the Hokuroku district, Akita prefecture, northeast Japan. *J. Geol. Soc. Japan* **107**, 354–357.

Tsukioka, S., Aoki, T., Yoshida, H., Hyakudome, T., Sawa, T., Ishibasi, S., Mizuno, M., Tahara, J. and Ishikawa, A. (2005) The PEM fuel cell system for autonomous underwater vehicles. *Mar. Tech. Soc. Japan* **39**, 56–64.

Yamashita, M., Kasaya, T., Takahashi, N., Takizawa, K. and Kodaira, S. (2015) Structural characteristics of the Bayonnaise Knoll caldera as revealed by a high-resolution seismic reflection survey. *Earth Planets Space*, **67**, 45, doi:10.1186/s40623-015-0214-2.